EAST EUROPEAN JOURNAL OF PHYSICS. 2. 600-609 (2026)
DOI:10.26565/2312-4334-2026-2-67 ISSN 2312-4334

THE THEORY OF THE IDEAL ARMOR PLATE. ENERGY REGULARITIES OF THE HIGH-SPEED BODY IMPACT ON AN ARMOR PLATE

M.P. Odeychuk, I.V. Tkachenko, V.I. Tkachenko*
National Science Center «Kharkiv Institute of Physics and Technology»,1 Akademicheskaya St., Kharkiv, 61108, Ukraine
**Corresponding Author e-mail: tkachenko@kipt.kharkov.ua*
Received January 14, 2026; revised March 20; 2026; accepted May 12, 2026

This study analyzes the optimal energy characteristics of a flying body (FB) impacting an armor plate (AP). The considered energy characteristics include momentum, kinetic energy, and the power of both bodies. It is shown that only a small fraction of the FB momentum is transferred to the AP, whereas nearly all of the FB kinetic energy is converted into the internal energy of the AP. This internal energy consists of the energy of mechanical oscillations of the plate and the energy associated with material displacement within it. The energy of the natural oscillations of the AP, modeled as a rectangular parallelepiped with dimensions a, b(with $a \sim b$) and thickness c, is estimated. The frequencies of bending oscillations perpendicular to and along the plate surface are calculated. It is shown that the energy of bending oscillations along the surface with the largest area exceeds that of oscillations perpendicular to the surface by a factor of a^2/c^2. The transfer of the FB kinetic energy is assumed to occur in a cylindrical channel of base area S_0. It is shown that the maximum power transferred from the FB to the AP is equal to $16/27 \approx 0.5926$ of the initial FB power and is accompanied by a reduction of the FB velocity by a factor of three. The characteristic penetration length corresponding to maximum power loss is proportional to the FB length h. The multilayer AP configuration is also considered. It is shown that in subsequent layers with lower material density, conditions for maximum power loss are preserved. The thickness of each layer is determined by the distance over which maximum power loss occurs. The results indicate that properly designed multilayer APs can significantly reduce overall dimensions and weight while maintaining high protective efficiency. It should be noted that the present analysis is qualitative and does not aim at quantitative agreement with experimental data, as some secondary effects are neglected. The results provide a physical basis for understanding energy dissipation mechanisms and suggest directions for further optimization using numerical methods.
Keywords: A*rmor plate; Flying body; Impact; Energy; Power loss; Multilayer*
PACS: 46.40.-f, 46.55.+d,81.40.Lm

INTRODUCTION

In recent years, due to the increasing number of military conflicts and localized hostilities, the problem of protecting personnel and equipment from high-speed projectiles has become especially relevant. This topic has been extensively studied and is widely covered in monographs, scientific publications, and textbooks. Typically, such works describe different types of ammunition, their key parameters, and their penetration capabilities (see, for example, [1–3]).

After introducing the properties of projectiles, various methods for analyzing their interaction with protective barriers are considered. One common approach is the use of empirical relationships derived from extensive experimental data on projectile impact and penetration. These relationships provide practical estimates of penetration depth and energy absorption.

In addition to empirical approaches, analytical models have been developed to describe projectile motion within a target as a combination of functions that account for projectile design, the barrier's material properties, and interaction conditions. Although such models can be reasonably accurate within their domain of applicability, they often remain closely related to empirical formulas and may be insufficient to solve advanced design problems.

Another important class of methods is based on continuum mechanics. These approaches rely on conservation laws of mass, momentum, and energy and are typically implemented using finite-difference or finite-element numerical techniques. Such methods provide a more physically grounded description of high-speed impact processes and allow detailed analysis of stress, deformation, and failure mechanisms.

Nevertheless, regardless of the modeling approach, experimental validation remains the primary criterion for assessing model accuracy. Numerous studies demonstrate that existing theoretical and numerical methods can adequately reproduce experimental results under appropriate conditions.

Modern research on improving the protective performance of armor systems increasingly focuses on multilayer and composite materials. For example, composite armor consisting of Al_2O_3 ceramics and ultra-high-molecular-weight polyethylene (UHMWPE) has demonstrated significant improvements in energy absorption [4]. Optimizing layer thickness and configuration can lead to substantial gains in ballistic resistance.

Similarly, studies of laminated aluminum alloys have shown that enhanced ballistic performance can be achieved by increasing energy dissipation through plastic deformation and delamination [5]. Lightweight protective structures based on aluminum alloys have also been proposed, with modeling approaches demonstrating good predictive capability under high strain-rate conditions [6].

A common drawback of many existing approaches is the need for extensive numerical computations to achieve optimal performance, particularly when maximizing energy absorption while minimizing weight. This limitation can be

Cite as: M.P. Odeychuk, I.V. Tkachenko, V.I. Tkachenko, East Eur. J. Phys. 2, 600 (2026), https://doi.org/10.26565/2312-4334-2026-2-67

addressed by introducing an additional optimization criterion that maximizes the projectile's power-loss rate during penetration.

The aim of the present work is to develop a theoretical framework for an ideal armor plate that maximizes the energy dissipation of a high-speed flying body. The proposed approach identifies key energy-loss mechanisms and establishes conditions under which the penetration depth is minimized while the projectile's power loss is maximized. This framework can serve as a basis for further refinement using numerical simulations and experimental validation.

1. GENERAL POSITIONS

When a flying object strikes an armored structure, the primary focus is on analyzing the structure's strength and reliability. AP with various geometric dimensions can serve as armored structures. The thickness, width, and height of APs can vary widely, but they generally have the form of rectangular parallelepipeds with a volume of $V = Sc$, where $S = ab$ is the maximum cross-sectional area of the AP, a and b are the length and width of the AP, respectively, and c is the thickness of the AP. The AP material is characterized by density $\rho = M/V$, where M is the mass of the AP.

The AP material is a single-layer or multi-layer metal plate whose elastic properties are characterized by Young's modulus E, strength by the tensile strength of the metal or its composition σ_B, and flow stress $\sigma_{0.2\%}$.

The FB is, in turn, also a metallic object, often of complex shape and composition. The FB is characterized by geometric dimensions comparable to the base plate's thickness. The volume of the FB has a cylindrical form and is equal to $V_0 = S_0 h$, where S_0 is the base of the cylinder and h is its height.

The density of the material FB is equal to $\rho_0 = m/V_0$, and the velocity is directed perpendicular to the maximum cross-sectional area AP and is equal to u_0.

In its simplest form, the FB material is a single-layer or multi-layer metal cylinder, the elastic properties of which are characterized by Young's modulus E^*. Strength is determined by the tensile strength of the cylinder's metal or metal composition σ_B^*, as well as the flow stress $\sigma_{0.2\%}^*$.

1.1. Energy Characteristics of the FB

The FB is characterized by the momentum M_{fb}:

$$M_{fb} = mu_0, \tag{1}$$

and kinetic energy W_{fb}:

$$W_{fb} = \frac{mu_0^2}{2}. \tag{2}$$

The power of the FB is determined by the expression:

$$P_{fb} = \frac{\rho_0 S_0 u_0^3}{2}. \tag{3}$$

The energy characteristics of the FB are momentum, kinetic energy and transferred power.

1.2. Processes of Transfer of Energy FB to Energy AP

The impact of the FB on the AP leads to an increase in the momentum and kinetic energy of the AP, as well as mechanical oscillations of the AP.

Furthermore, there will be an increase in the AP temperature in the region of the FB's impact, limited to an area of approximately S_0. This localized temperature increase has been confirmed in many experiments studying the impact of the FB on the AP (see, for example, [3]). The localized temperature increase is so great that over an area of approximately S_0, the metal liquefies. In this case, we will consider a situation in which the depth of metal melting is approximately equal to the AP thickness. Otherwise, the AP is not pierced, and it performs its intended function. Therefore, we will not consider this case further.

Based on the above, when analyzing the energy characteristics of the AP, we will assume that two energy absorption processes are occurring simultaneously.

One process involves the absorption of energy by the entire volume of AP.

The second process is associated with the absorption of energy by the FB in a cylindrical channel of area S_0.

1.3. Transfer of the FB Energy into Oscillatory Energy of the Entire AP Volume

When FB impacts an AP, its kinetic parameters must be analyzed. These include the AP's momentum, kinetic energy, and power.

The AP's momentum M_{ap} is determined by the expression:

$$M_{ap} = Mw \tag{4}$$

where w is the AP velocity.

The kinetic energy of the AP W_{ap} is equal to:

$$W_{ap} = \frac{Mw^2}{2}. \tag{5}$$

The power of the AP P_{ap} is determined by the formula:

$$P_{ap} = \frac{\rho S w^3}{2}. \tag{6}$$

To determine the energy of mechanical oscillations of bending AP, we will proceed from the fact that the oscillations are subject to a rectangular plate with supported edges, whose edges only rest on a fixed support, but are not attached to it. We will determine the lowest frequency ω_{ap} of the bending oscillations of a rectangular plate for a neutral surface on which there is no tension. We will define the shape of the neutral surface by the expression $\zeta(x, y, t) = h_{ap} sin(k_x x) sin(k_y y) sin(\omega_{ap} t)$, where h_{ap} is the bending amplitude, $k_x = \pi/a$, $k_y = \pi/b$ are the wave numbers of oscillations in the x and y directions, $\omega_{ap} = 2\pi/T$, T is the period of the bending oscillations of the AP [7]. The magnitude of the frequency ω_{ap} is determined by the expression:

$$\omega_{ap} = \sqrt{\frac{Ec^2}{12\rho(1-\nu^2)}}\left[\left(\frac{\pi}{a}\right)^2 + \left(\frac{\pi}{b}\right)^2\right], \tag{7}$$

where ν is Poisson's ratio.

From [7], we determine the average kinetic energy of bending oscillations AP over the oscillation period T. It is determined by the expression:

$$\Omega_{ap} = \frac{\pi^4}{192}\frac{Ec^3 h_{ap}^2}{(1-\nu^2)}\left(\left(\frac{1}{a}\right)^2 + \left(\frac{1}{b}\right)^2\right)^2 ab, \tag{8}$$

Deviations of the surface of the AP from the equilibrium position caused by mechanical oscillations lead to an elongation ε, the value of which is determined by the expression:

$$\varepsilon = \frac{\pi}{4}\frac{h_{ap}^2}{a^2}. \tag{9}$$

Expression (8) allows us to determine the plasticity region of each AP, since exceeding the critical elongation value can lead to AP failure. In each specific case, such calculations must be performed to assess the AP's shape retention.

2. ENERGY TRANSFER FROM THE FB

When considering the energy transfer of the FB to AP, it is always important to know the answers to the following questions:

1. What is the minimum initial penetration velocity of the AP.
2. What changes in momentum and energy occur between interacting objects.
3. What are the conditions for loss of maximum power by FB.
4. What are the requirements for the multilayer AP?

Some of these questions are answered in the dissertation [8] and in the monograph [3].

In the dissertation [8], a general concept for barrier penetration is defined based on an analysis of high-velocity impact processes and armor penetration of various materials. This concept is based on the principle of redistributing the kinetic energy of an impact between the surface area of contact and the barrier's deep penetration. Using the proposed concept, the effects of ultra-deep penetration of micro-impactors under critical impact conditions are described.

However, the data in [3, 8] and many other sources not cited in this paper are not always readily available and require additional calculations. Therefore, answers to the questions posed are proposed below, formulated based on conservation laws.

2.1. A Minimum Initial AP Penetration Velocity

Based on the strength characteristics of the AP and the energy parameters of the FB, it is possible to formulate a condition for AP penetration. This condition is the requirement that the FB pressure on the AP surface exceeds the resistance force, which is determined by the flow stress $\sigma_{0.2\%}$:

$$\frac{1}{2}\rho_0 u_0^2 > \sigma_{0.2\%}. \tag{10}$$

To inequality (10) it is necessary to add the condition of smallness of the speed FB compared to the speed of sound c_s in the material AP:

$$u_0 < c_s. \tag{11}$$

From (10) and (11) we obtain the condition for the value of the speed FB at which the penetration of the AP occurs:

$$u_{0,min} = \frac{2\sigma_{0.2\%}}{\rho_0 c_s} < u_0 < c_s \tag{12}$$

The minimum speed $u_{0,min}$ of penetration of the AP is determined by the lower limit of inequality (12).

2.2. The Momentum and Energy of Interacting Objects Changing

The kinetic energy and momentum of the FB will be transferred to the entire AP, as well as to the material located in a cylindrical channel of area S_0. When the FB impacts the material in a cylindrical channel of area S_0, it can be assumed that a cork is formed, which can be squeezed out of the AP volume. Due to various dissipative processes (viscosity, thermal heating, and friction of the cork against the walls of the cylindrical channel), incomplete energy and momentum transfer between the FB and the cork should be observed.

Due to the high energy of the FB and the significant difference in the masses of the AP and FB, it can be concluded that the laws of conservation of energy and momentum are approximately satisfied. In a perfectly inelastic collision, the velocity of the AP after the interaction is equal to $\widehat{w}$ and is determined by the expression:

$$\widehat{w} \approx \frac{m}{(m+M)} u_0. \tag{13}$$

In a perfectly inelastic collision, the FB gets stuck in the AP, and the FB loses kinetic energy ΔW:

$$\Delta W = \frac{m u_0^2}{2} - \frac{(m+M)\widehat{w}^2}{2} = \frac{M}{M+m}\frac{m u_0^2}{2}. \tag{14}$$

Since $m \ll M$, practically all kinetic energy is converted into internal energy of the AP. The ratio $M/(M+m)$ determines the proportion of the FB kinetic energy converted into internal energy AP.

2.3. Conditions for Maximum Power Loss of the FB

To evaluate the efficiency of AP use, it is necessary to determine the conditions under which the FB power loss is maximum. For this, we will consider the energy exchange per unit of time between the FB and the cork in a cylindrical channel AP of area S_0.

Per unit of time, the following mass passes through the area S_0:

$$\dot{m} = \rho_0 S_0 u_0^{'}, \tag{15}$$

where $u_0^{'}$ is an average speed FB, and the dot above the letter means the time derivative.

The power transferred to the cork is estimated by the value:

$$P_{cork} = \frac{\dot{m}}{2}\left(u_0^2 - u_{0,fin}^2\right), \tag{16}$$

where $u_{0,fin}$ is the final velocity of the FB in the channel.

At the same time, the power consumption of the FB can be defined as the product of the resistance force F and the average speed of the FB:

$$P_{fb}^{'} = F u_0^{'}, \tag{17}$$

The resistance force can be estimated by the value:

$$F = \dot{m}\left(u_0 - u_{0,fin}\right), \tag{18}$$

From (16), (17), and (18) it follows that the average speed is equal to:

$$u_0^{'} = \frac{1}{2}\left(u_0 + u_{0,fin}\right). \tag{19}$$

From (16), we obtain a function that describes the dependence of the FB power on the speed together with the cork:

$$\begin{aligned} P_{cork} &= \frac{1}{2}\rho_0 S_0 u_0^{'}\left(u_0^2 - u_{0,fin}^2\right) = \frac{1}{2}\rho_0 S_0 \frac{1}{2}\left(u_0 + u_{0,fin}\right)\left(u_0^2 - u_{0,fin}^2\right) \\ &= \frac{1}{4}\rho_0 S_0 u_0^3 \left(1 + \frac{u_{0,fin}}{u_0}\right)\left(1 - \frac{u_{0,fin}^2}{u_0^2}\right). \end{aligned} \tag{20}$$

Analysis (20) shows that the maximum power will be transferred to the cork in a cylindrical channel provided that the final velocity satisfies the condition: $u_{0,fin} = u_0/3$. In this case, the lost power FB is equal to:

$$(P_{cork})_{max} = \frac{1}{2}\rho_0 S_0 u_0^3 \frac{16}{27} = \eta \cdot (W_{cork})_0. \tag{21}$$

where $(P_{cork})_0 = \rho_0 S_0 u_0^3\,/2$ is the initial power of FB, $\eta = 16/27 \approx 0.5926$ is the power transfer coefficient.

The coefficient η coincides with the condition of A. Betz, which determines the maximum efficiency of a wind turbine [9].

Let us determine the distance at which this velocity FB decreases by a factor of three, i.e. $u_{0,fin} = u_0/3$. To do this, we write the equation of displacement of the contact boundary of FB of mass m with the cork:

$$\frac{du_0}{dt} = -\frac{1}{h}\left(u_0 + u_{0,fin}\right)\left(u_0 - \frac{1}{2}u_{0,fin}\right) \tag{22}$$

Using the substitution $t = x/u_{0,fin}$, where x is the coordinate of the location of the contact boundary of the FB with the cork, we transform the equation to the form:

$$\frac{dy}{dx} = -\frac{1}{h}(y+1)\left(y - \frac{1}{2}\right) \tag{23}$$

where $y = u_0/u_{0,fin}$.

The solution to equation (23) is a function of the form:

$$y(\xi) = \frac{1}{2}\frac{\left(1 + 2e^{-\frac{3}{2}(\xi+\xi_0)}\right)}{\left(1 - e^{-\frac{3}{2}(\xi+\xi_0)}\right)} \tag{24}$$

where $\xi = x/h$ is the distance at which the FB loses its maximum power, ξ_0 is the integration constant.

The constant ξ_0 is determined from the condition that $y(\xi)$ should change three times over the distance of maximum power loss, for example, from $y(0) = 3^{n+1}$ to $y(z_{1,n}) = 3^n$, where the condition $n \gg 1$ must be fulfillment.

Calculations using formula (24) show that a decrease in the initial velocity FB by 3 times is observed at a distance of:

$$z_{1,n} = \frac{2}{3}ln\left[\frac{(3^n+1)}{(3^n-0.5)}\frac{(3^{n-1}-0.5)}{(3^{n-1}+1)}\right] \tag{24, a}$$

Thus, a threefold decrease in speed with a maximum loss of power FB occurs at a distance $x_n = z_{1,n}h$, where n is selected based on the realism of the obtained distance and experimental data.

2.4. Requirements for Ideal Multilayer AP

Ideal multilayer APs are those that provide maximum FB power loss. To calculate the ideal AP, for example, we'll compile Table 1, which lists the characteristic FB and AP parameters.

Table 1. Mass, geometric, strength, kinematic and energy characteristics of FB and AP

Parameter name	AP	FB
Mass, *kg*	M	m
Base area, *m*^{2}	$S = ab, (a -$ length$, m;\ b -$ width$, m)$	S_0
Thickness/length, *m*	c	h
Volume, *m*^{3}	$V = Sc$	$V_0 = S_0 h$
Density, *kg*/*m*^{3}	ρ	ρ_0
Young's modulus, *MPa*	E	E^*
Tensile strength, *MPa*	σ_B	σ_B^*
Flow stress, *MPa*	$\sigma_{0.2\%}$	$\sigma_{0.2\%}^*$
Velocity, *m/s*	w	u_0
Momentum, *kg*· *m*/s	M_{ap}	M_{fb}
Kinetic energy, *J*	W_{ap}	W_{fb}
Power, *kg*·*m*^{2}/*s*^{3}	P_{ap}	P_{fb}

When describing the impact of the FB on the AP, we distinguish two main processes:
- transfer of the FB momentum and energy to the entire volume of the AP;

- transfer of the FB energy to the AP material in a cylindrical channel of area S_0, which is formed by the high-energy pulsed impact of the FB on the AP.

The energy indicators of these processes are summarized in Table 2, where the characteristic indicators of energy transfer FB to the entire volume of the AP (Transfer I) and the characteristic indicators of energy transfer FB in the AP in a cylindrical channel with the base S_0 (Transfer II) are highlighted.

Table 2. Characteristic indicators of optimal energy transfer from the FB to the AP

Parameter name	Transfer I	Transfer II
Frequency of mechanical oscillations of bending of a rectangular plate, *s*$^{-1}$	ω_{ap}	–
Amplitude of mechanical oscillations of the AP bending, *m*	h_{ap}	–
Energy of bending AP oscillations with amplitude h_{ap}, *kg·* m^2/s	Ω_{ap}	–
Elongation due to mechanical oscillations AP, dimensionless	ε	–
Velocity, *m/s*	$\widehat{w} \ll u_0$	u_0
Power, *kg·* m^2/s^3	$P_{ap} \ll P_{fb}$	P_{cork}
Final speed of the FB at maximum power transfer, *m/s*	–	$\frac{1}{3}u_0$
One-time distance of maximum power loss of the FB, *m*	–	$z_{0,n}h$

The previous section described the conditions for the loss of maximum power FB in a single-layer AP, which corresponds to the ideal single-layer AP.

Below we will consider the requirements for ideal multilayer AP.

From (24) it follows that for a given n, at a distance $z_1 = z_{1,n}$, the maximum power loss of the FB is observed. For a single-layer AP, this power loss may be insufficient, and the FB will continue its movement with an undesirable result. Therefore, the question arises of using a second, and if that doesn't help, a third, or even more layers of AP. The answer to this question is contained in the results obtained for the first AP layer.

The expression for the maximum power loss (21) contains only the material density FB, the cross-section, and the velocity of the FB. Therefore, to estimate the optimal distance for the loss of maximum power in the second layer, the previous consideration is applicable, where a threefold decrease in the velocity of the FB with the loss of maximum power will already occur at a distance $z_2 = z_{1,n-1}$.

Fig. 1 shows a diagram for calculating the location of the first two layers of the AP when the FB passes with an initial velocity u_0 with a AP thickness equal to c. Position I is the moment the FB enters the AP, position II is the moment the first layer of the AP with thickness z_1 is formed, position III is the moment the second layer of the AP with thickness z_2 is formed.

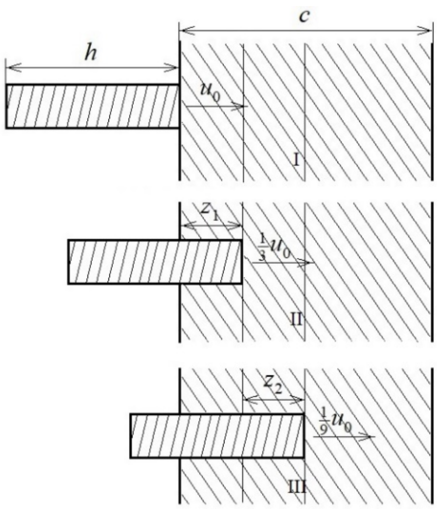

Figure 1. Schematic diagram of the arrangement of the first two layers of the AP as the FB of length h passes with an initial velocity u_0 at AP thickness equal to c

In the third layer of the AP, a threefold decrease in speed will occur at a distance $z_3 = z_{1,n-2}$.

Summing up these distances, we obtain the total thickness of the N - layer AP, at which the speed of the FB will change by 3^N times:

$$x_n \approx z_{1,n} + z_{1,n-1} + z_{1,n-2} + \cdots \quad (25)$$

Thus, for example, for $n = 4$ and for a three-layer AP ($N = 3$), there is a 27-fold decrease in the velocity of the FB over a length of $x_3 = 0.024 + 0.072 + 0.205 = 0.301$ and a loss of $\Delta U_3 = \eta + (1 - \eta)\,\eta + (1 - \eta - (1 - \eta)\,\eta)\,\eta \approx 0.932$ of the part of the initial power of the FB.

If the number of layers is large, i.e. $n \gg 1$, then the total power loss of the FB tends to unity, since the power losses in layers are determined by the expressions:

1 layer – η;

2 layer - $(1 - \eta)\,\eta$;

3 layer - $(1 - \eta - (1 - \eta)\,\eta)\,\eta$;

4 layer - $(1 - \eta - (1 - \eta)\,\eta - (1 - \eta - (1 - \eta)\,\eta)\,\eta)\eta$;

The total power loss is determined by an infinite decreasing geometric progression:

$$\Delta P_{n\to\infty} = \eta + (1 - \eta)\,\eta + (1 - \eta - (1 - \eta)\,\eta)\,\eta + (1 - \eta - (1 - \eta)\,\eta - (1 - \eta - (1 - \eta)\,\eta)\,\eta)\eta$$
$$+ \cdots = \eta[1 + (1 - \eta) + (1 - \eta)^2 + (1 - \eta)^3 + \cdots] = \eta\frac{1}{1 - (1 - \eta)} = 1.$$

From the calculations carried out it follows that in order to lose the maximum power of the FB in a multilayer AP, it is necessary to select the thickness of the layers in accordance with (25), where each term determines the thickness of the layers from the first $z_{0,n}$ to the second $z_{0,n-1}$, the third $z_{0,n-2}$, and so on.

For example, for an initial velocity of the FB 600 *m/s* and a minimum penetration velocity of 58.5 *m/s*, calculated using formula (12), it is sufficient to use a two-layer AP, since in a two-layer AP the velocity of the FB decreases by 9 times.

Since the density of the AP material is not included in the calculation of maximum power loss, subsequent layers of the AP can be composed of a lower-density material to lighten the structure. The optimal number and sequence of lightweight layers placed after the first layer should be determined experimentally.

3. NUMERICAL ESTIMATES OF THE IMPACT OF FB ON AP

Let us present numerical estimates of FB's impact on the AP. The initial data will be the average FB velocities and the characteristic AP parameters corresponding to the 7.62 *mm* AKM 7.62 *mm* PS bullet of the 1943 model 57-H-231 cartridge in a steel shell with a steel core, weight 7.9 *g*, with an initial velocity of 730 *m/s* [3].

As stated above, the FB has two channels of momentum, energy, and power loss.

These losses are as follows:

- losses due to the transfer of momentum and energy of the FB to the entire volume of the power supply.
- losses caused by the transfer of energy FB to the AP material in a cylindrical channel with the base S_0. The channel is formed by the high-energy pulsed action of the FB on the AP.

Let's first estimate the momentum and energy transfer of the FB to the entire volume of the AP. We'll assume that the angle α between the FB axis and the normal to the AP is equal to zero. Increasing this angle increases the AP thickness and improves the APs protective properties. Table 3 presents the characteristic parameters of the FB and AP steel, taken from [3].

Table 3. Characteristic mass, geometric, strength, kinematic, and energy parameters of FB and AP

Parameter name	AP	FB
Mass, *kg*	$M = 2.18$	$m = 7.9 \cdot 10^{-3}$ 7.62mm Kalashnikov assault rifle (AKM), steel core
Base area, *m*^{2}	$S = ab = 0.2 \times 0.2 = 4 \cdot 10^{-2}$, ($a$ – length, м; b – width, м)	$S_0 = 4.56 \cdot 10^{-5}$
Thickness, м	$c = 7 \cdot 10^{-3}$	$h = 2.68 \cdot 10^{-2}$
Volume, *m*^{3}	$V = Sc = 2.8 \cdot 10^{-4}$	$V_0 = S_0 h = 1.22 \cdot 10^{-6}$
Density, *kg/m*^{3}	$\rho = 7810$	$\rho_0 = 7810$
Young's modulus, *MPa*	$E = 2.15 \cdot 10^5$	$E^* = 2.15 \cdot 10^5$
Tensile strength, *MPa*	$\sigma_B = 30060$	$\sigma_B^* = 30060$
Flow stress, *MPa*	$\sigma_{0.2\%} = 1370$	$\sigma_{0.2\%}^* = 1370$
Poisson's ratio,	$\sigma = 0.33$	$\sigma = 0.33$
Rate of plastic deformation, *s*$^{-1}$	$\dot{\varepsilon} = 5 \cdot 10^4$	$\dot{\varepsilon} = 5 \cdot 10^4$
Sound velocity, *m/s*	$c_s = 5900 \ldots 6100$	$c_s = 5900 \ldots 6100$

Parameter name	**AP**	**FB**
Velocity, *m/s*	$w = 0$	$u_0 = 600 \cdots 745$
Momentum, *kg· m/s*	$M_{ap} = 0$	$M_{fb} = 4.74 \ldots 5.9$
Kinetic energy, *kJ*	$W_{ap} = 0$	$W_{fb} = 1.422 \ldots 2.192$
Power, *MW*	$P_{ap} = 0$	$P_{fb} = 38.5 \ldots 73.6$

It should be noted that given such a huge energy input and the rapidity of the processes, not all the coefficients in Table 3 are valid. However, we will assume that they are of the same order of magnitude. The true values of these coefficients must be determined experimentally.

4. TRANSFER OF THE FB ENERGY INTO ENERGY OF THE ALL VOLUME OF THE AP

Penetration and energy transfer from the FB to the energy of the entire volume of the AP is possible at a velocity FB satisfying condition (12). In numerical expression for the parameters of Table 3, this velocity value must satisfy the inequality:

$$58.5 < u_0 < 6000, m/s. \tag{26}$$

From the law of momentum conservation, we estimate the acquired speed by the AP:

$$\widehat{w} = \frac{7.9 \cdot 10^{-3} \cdot 600}{2.18} \approx \frac{mu_0}{M} = 2.17, m/s \tag{27}$$

Thus, the displacement of the AP during the incident is of the order of $\widehat{w}/\dot{\varepsilon} \sim 10^{-5}$ *m* and represents a very small value. The acquired kinetic energy of the AP is of the order of:

$$W_{ap} = \frac{M\widehat{w}^2}{2} \approx 1.09 \cdot 4.7 \approx 5.13, \qquad J. \tag{28}$$

The power received from the FB to the AP is determined by the value:

$$P_{ap} = \frac{M\widehat{w}^3}{2c} \approx \frac{2.18 \cdot 10.22}{2 \cdot 7 \cdot 10^{-3}} = 1.59 \cdot 10^3, \ W. \tag{29}$$

The kinetic energy (28) and power (29) acquired by the AP are small values relative to the initial values for FB: $W_{fb} \approx 0.5 \cdot 7.9 \cdot 10^{-3} 600^2 = 1.422$ *kJ* and $P_{fb} \approx 0.5 \cdot 7.810 \cdot 4.56 \cdot 10^{-2} 600^3 \approx 3.85 \cdot 10^7$ *W*. Therefore, the change in the kinetic energy (28) and power (29) of the AP can be ignored when analyzing the energy exchange between the FB and the AP.

As shown above, the analysis of energy exchange between the FB and the AP includes an estimate of the power (21) converted into the AP's internal energy and an estimate of the distance over which this transition occurs (24).

A certain portion of the FB kinetic energy is also converted into the internal energy of the mechanical oscillations of the AP. Below, we present a numerical estimate of the energy and associated parameters transferred to the AP's mechanical oscillations.

4.1. Elongation, Frequency, and Energy of Mechanical Bending Oscillations According to Thickness *c*

Below, based on formulas (7), (8), (9), and the data in Table 3, are numerical estimates of the elongation (30.1), frequency (30.2), and energy of mechanical oscillations of bending across thickness c (30.3) under the condition $a \sim b$:

$$\varepsilon_c = \frac{\pi}{4} \frac{h_{ap}^2}{a^2}, \tag{30.1}$$

$$\omega_{ap} = \sqrt{\frac{Ec^2}{12\rho(1-\nu^2)}} \left[\left(\frac{\pi}{a}\right)^2 + \left(\frac{\pi}{b}\right)^2 \right] = 5.546 \cdot 10^3, \ s^{-1} \tag{30.2}$$

$$\Omega_{ap} = 2.03 \frac{2.15 \cdot 10^5 (7 \cdot 10^{-3})^3}{(1-0.89)} \frac{h_{ap}^2}{4 \cdot 10^{-2}} \approx 1.68 \cdot 10^5 \frac{h_{ap}^2}{a^2} = 1.68 \cdot 10^5 \frac{4}{\pi} \varepsilon_c, \qquad J. \tag{30.3}$$

In addition to mechanical bending oscillations along thickness c, similar flexural vibrations may also exist along length a. In this case, the elongation, frequency, and energy of the mechanical bending oscillations are described by other expressions. Let's define these expressions and perform numerical estimates of their values.

4.2. Elongation, Frequency, and Energy of Mechanical Bending Oscillations According to Thickness a

The elongation (31.1), frequency (31.2) and energy of mechanical bending oscillations along the length a (31.3) can be obtained from (7), (8), (9), if we replace $a \to c$ and $c \to a$ in them. Finally, under the condition $a \sim b$, we obtain numerical estimates of the indicated quantities:

$$\varepsilon_a = \frac{\pi}{4}\frac{h_{ap}^2}{c^2}, \tag{31.1}$$

$$\omega_{ap} = \sqrt{\frac{Ea^2}{12\rho(1-\nu^2)}}\left[\left(\frac{\pi}{c}\right)^2 + \left(\frac{\pi}{b}\right)^2\right] \approx \sqrt{\frac{Ea^2}{12\rho(1-\nu^2)}}\left(\frac{\pi}{c}\right)^2 =$$
$$= \sqrt{\frac{2.15\cdot 10^{11}\cdot 4\cdot 10^{-2}}{12\cdot 7810\cdot (0.89)}}\left(\frac{\pi}{7\cdot 10^{-3}}\right)^2 = \sqrt{\frac{2.15\cdot 10^{6}\cdot 4}{12\cdot 7.810\cdot 0.89}}10^6\cdot 0.2 = 6.42\cdot 10^7,\ s^{-1} \tag{31.2}$$

$$\Omega_{ap} = \frac{\pi^4}{192}\frac{Ea^3h_{ap}^2}{(1-\nu^2)}\left(\left(\frac{1}{c}\right)^2 + \left(\frac{1}{a}\right)^2\right)^2 ca \approx \frac{\pi^4}{192}\frac{Ea^3h_{ap}^2}{(1-\nu^2)}\left(\frac{1}{c}\right)^4 ca = \frac{\pi^4}{192}\frac{Ea^4h_{ap}^2}{(1-\nu^2)}\left(\frac{1}{c}\right)^3 =$$
$$= \frac{\pi^4}{192}\frac{Ea^4}{(1-\nu^2)c}\frac{h_{ap}^2}{c^2} \approx \frac{\pi^4}{192}\frac{2.15\cdot 10^{11}\cdot 2^4\cdot 10^{-4}}{(0.89)\cdot 7\cdot 10^{-3}}\frac{h_{ap}^2}{c^2} \approx 2.8\cdot 10^{10}\frac{h_{ap}^2}{c^2} = 2.8\cdot 10^{10}\frac{4}{\pi}\varepsilon_a, \quad J. \tag{31.3}$$

In (30.1), (30.3), (31.1), (31.3), unknown quantities are elongations $\varepsilon_{a,c}$. Their values can be estimated by comparing the initial kinetic energy of the FB $W_{fb} \approx 1.422\ kJ$ and the energy of mechanical bending oscillations across the thickness c or a:

From (32) it follows that the elongation of mechanical bending oscillations along the thickness c is greater than that along the length a. It is obvious that it is these vibrations that are responsible for the mechanical destruction of the AP, since for certain grades of steel, elongations of the order of several percent are destructive [10].

CONCLUSIONS

The conditions for realizing an ideal armor plate (AP) under impact by a flying body (FB) have been investigated. As an illustrative example, an AP with a mass of $M = 2.18$ kg subjected to the impact of a 7.62 mm projectile with a mass of $m = 7.9 \times 10^{-3}$ kg has been analyzed. Although this specific case is considered, the proposed approach can be extended to other types of projectiles and target materials. The study focuses on the transformation of the FB energy characteristics - momentum, kinetic energy, and power - during interaction with the AP. It is shown that only a small fraction of the FB momentum is transferred to the AP, while nearly all of the FB kinetic energy is converted into the internal energy of the plate. This internal energy consists of the energy of mechanical oscillations of the entire plate and the energy associated with material displacement within it. The AP is modeled as a rectangular parallelepiped with dimensions a, b(with $a \sim b$) and thickness c. The frequencies of natural bending oscillations perpendicular to and along the plate surface have been estimated. It is shown that oscillations along the surface with the largest area occur in the megahertz range, whereas oscillations perpendicular to the surface lie in the kilohertz range. The energy of bending oscillations along the surface exceeds that of perpendicular oscillations by a factor of a^2/c^2. Under the condition $a^2/c^2 \gg 1$, this may lead to significant tensile strains and potential cracking of the plate. The analysis demonstrates that the ratio $M/(M+m)$ determines the fraction of the FB kinetic energy converted into the internal energy of the AP, which approaches unity for $m \ll M$. The transfer of kinetic energy is assumed to occur in a cylindrical channel of base area S_0. It is shown that the maximum power transferred from the FB to the AP reaches $16/27 \approx 0.5926$ of the initial FB power and corresponds to a reduction of the FB velocity by a factor of three. For normal impact, the characteristic penetration length over which maximum power loss occurs is proportional to the FB length h. The multilayer AP configuration has also been analyzed. It is shown that in subsequent layers with lower material density, the conditions for maximum power loss remain similar to those in the first layer. The optimal thickness of each layer is determined by the distance over which the FB experiences maximum power loss. The results indicate that properly designed multilayer armor plates can significantly reduce overall dimensions and weight while maintaining high protective performance. It should be emphasized that the present analysis is qualitative and does not aim to directly quantify agreement with experimental data, as several secondary effects have not been taken into account. Nevertheless, the proposed approach provides a physical basis for understanding energy dissipation mechanisms and offers guidance for further optimization using numerical modeling and experimental validation.

ORCID
Mikola Odeychuk, https://orcid.org/0000-0002-6507-2588; **Ivan Tkachenko,** https://orcid.org/0009-0005-1378-2077;
Viktor Tkachenko, https://orcid.org/0000-0002-1108-5842

REFERENCES

[1] I. A. Balaganskii, and L. A. Merzhievskii, *The action of weapons and ammunition*, (Izd-vo NGTU, Novosibirsk, 2004). (in Russian)
[2] V. M. Fomin, A. I. Gulidov, G. A. Sapozhnikov, *et al.*, *High-speed interaction of bodies*, (Izd-vo Sib. otd-niia Ros. akad. nauk, Novosibirsk, 1999). (in Russian)
[3] S. A. Manzhura, D.S. Baulin, S.A. Gorєlishev, *et al.*, *Multilayer armored structures to provide protection for personnel and military equipment*, (NA NGU, Kharkiv, 2023). (in Ukrainian)
[4] W. Lu, Y. Wu, M. Ma, Y. Yu, X. Zhou, and G. Gao, Theoretical and Applied Mechanics Letters, **14**(5), 100550 (2024). https://doi.org/10.1016/j.taml.2024.100550
[5] F. Min, K. Gao, W. Wei, X. Wu, S. Wen, H. Huang, Z. Nie, *et al.*, Int. J. Impact Eng. **191**, 104998 (2024). https://doi.org/10.1016/j.ijimpeng.2024.104998
[6] Y. Wu, W. Lu, Y. Yu, M. Ma, X. Sun, and G. Gao, Solids, **60**, 2695 (2025). https://doi.org/10.1134/S0025654425601624
[7] L. D. Landau, and E. M. Lifshitz, *Theory of elasticity,* (Pergamon Press, Oxford, 1986).
[8] S. E. Aleksentseva, Dr.S. dissertation, Samara, 2015. (in Russian)
[9] A. Betts, UFN, **10**(2), 26 (1930). (in Russian)
[10] A. V. Darkov, and G. S. Shapiro, *Strength of materials*, (Vysshaia shkola, M., 1975). (in Russian)

ТЕОРІЯ ІДЕАЛЬНОЇ БРОНЕВОЇ ПЛИТИ. ЕНЕРГЕТИЧНІ ЗАКОНОМІРНОСТІ УДАРУ ВИСОКОШВИДКІСНОГО ТІЛА ПО БРОНЕВІЙ ПЛИТІ

М.П. Одейчук, І.В. Ткаченко, В.І. Ткаченко
Національний науковий центр «Харківський фізико-технічний інститут», вул. Академічна, 1, Харків, 61108, Україна

Це дослідження присвячено аналізу оптимальних енергетичних характеристик летючого тіла (ЛТ), що зіткнеться з броньовою пластиною (БП). Розглянуті енергетичні характеристики включають імпульс, кінетичну енергію та потужність обох тіл. Показано, що лише невелика частина імпульсу ЛТ передається БП, тоді як майже вся кінетична енергія ЛТ перетворюється на внутрішню енергію БП. Ця внутрішня енергія складається з енергії механічних коливань пластини та енергії, пов'язаної зі зміщенням матеріалу всередині неї. Оцінено енергію власних коливань ЛТ, змодельованого як прямокутний паралелепіпед з розмірами a, b де $a \sim b$ та товщиною c. Розраховано частоти згинальних коливань, перпендикулярних поверхні пластини та вздовж неї. Показано, що енергія згинальних коливань вздовж поверхні з найбільшою площею перевищує енергію згинальних коливань, перпендикулярних до поверхні, в a^2/c^2 разів. Вважається, що передача кінетичної енергії ЛТ відбувається в циліндричному каналі з площею основи S_0. Показано, що максимальна потужність, що передається від ЛТ до БП, дорівнює 16/27≈0,5926 від початкової потужності ЛТ та супроводжується зменшенням швидкості ЛТ утричі. Характерна довжина проникнення, що відповідає максимальним втратам потужності, пропорційна довжині ЛТ h. Також розглянуто багатошарову конфігурацію БП. Показано, що в наступних шарах з меншою щільністю матеріалу зберігаються умови для максимальних втрат потужності. Товщина кожного шару визначається відстанню, на якій відбуваються максимальні втрати потужності. Результати показують, що правильно спроєктовані багатошарові БП можуть значно зменшити габаритні розміри та вагу, зберігаючи при цьому високу захисну ефективність. Слід зазначити, що цей аналіз є якісним і не має на меті забезпечити кількісну відповідність експериментальним даним, оскільки деякі вторинні ефекти не враховуються. Результати забезпечують фізичну основу для розуміння механізмів дисипації енергії та пропонують напрямки подальшої оптимізації за допомогою числових методів.
Ключові слова: *броньова плита; літаюче тіло; удар; енергія; втрати потужності; багатошаровість*